Nuclear Instruments and Methods in Physics Research A 858 (2017) 57–61

Contents lists available at ScienceDirect

Nuclear Instruments and Methods in Physics Research A

journal homepage: www.elsevier.com/locate/nima

# Baseline restoration technique based on symmetrical zero-area trapezoidal pulse shaper

Guoqiang Zeng[a], Jian Yang[a,*], Tianyu Hu[a], Liangquan Ge[a], Xiaoping Ouyang[b], Qingxian Zhang[a], Yi Gu[a]

[a] Key Laboratory of Applied Nuclear Techniques in Geosciences Sichuan, Chengdu University of Technology, Chengdu 610059, China
[b] Northwest Institute of Nuclear Technology, Xi'an 710024,China

ARTICLE INFO

*Keywords:*
Baseline restoration
Symmetrical zero-area
Pulse shaping
Digital signal processing

ABSTRACT

Since the baseline of the unipolar pulse shaper have the direct-current (DC) offset and drift, an additional baseline estimator is need to obtain baseline values in real-time. The bipolar zero-area (BZA) pulse shapers can be used for baseline restoration, but they cannot restrain the baseline drift due to their asymmetrical shape. In this study, three trapezoids are synthesized as a symmetrical zero-area (SZA) shape, which can remove the DC offset and restrain the baseline drift. This baseline restoration technique can be easily implemented in digital pulse processing (DPP) systems base on the recursive algorithm. To strengthen our approach, the iron's characteristic x-ray was detected using a Si-PIN diode detector. Compared with traditional trapezoidal pulse shapers, the SZA trapezoidal pulse shaper improved the energy resolution from 237 eV to 216 eV for the 6.403 keV Kα peak.

## 1. Introduction

Many pulse shaping methods are used to improve the energy resolution and the stability of radiation measurement systems, such as the Gaussian shaper, trapezoid shaper, cusp-like shaper and 1/f shaper [1–3]. Since these methods are unipolar in shape and are not zero-area, The DC offset and drift exist in the baseline of the pulse shaping. Therefore, a baseline restorer should be designed to accurately extract the peak location of the pulse signals. The optimum baseline filter theory have been discussed in some literatures [4,5]. Some digital baseline restorers are also already implemented in the digital systems and even can be used in high count rates systems [6–9]. But these baseline restoration approach may be more complex than their pulse shaping.

The baseline filter and restoration method of the zero-area pulse shaping have been mentioned have been mentioned in the reference [10]. But it cannot be easily implemented in the digital systems. Ref. [11] studied the bipolar triangular shaper for pile-up correction. Since the triangular shape is not a zero-area, its baseline would have serious undershoot at the pulse pile-up. The BZA trapezoidal shaper for neutron-gamma discrimination was studied in Ref. [12], which used the flat-top to determine the neutron and gamma signals. Due to its zero-area shape, the BZA trapezoidal shaper can be used for baseline restoration, but cannot restrain the baseline drift. The BZA cusp-like shaper, which is also not a symmetrical shape, was studied in Ref. [13]. In this work, we use an simplest SZA trapezoidal shape based on the extensively applied trapezoidal shaper. Its zero-area shape can be used for baseline restoration, and its symmetrical shape can automatically eliminate the baseline drift. Most of all, It can be easily implemented in field programmable gate array (FPGA) and only need a little logic element by the recursive algorithm.

## 2. Method of the baseline restoration

The exponential signal is a typical output of a nuclear detector. The digital signal processing method of the exponential signal using a traditional trapezoidal pulse shaper is shown in Fig. 1 [14]. The analog pulse signal is digitized by the high-speed ADC, and then the digital pulse signal is deconvoluted to remove the exponential tails in order to obtain a unit impulse signal. Finally, the unit impulse signal is put into the synthesis system of the pulse shaping. Since the input of the synthesis system is the unit impulse signal, $\delta[n]$, the output of the trapezoidal shaper is merely the transfer function $h_X[n]$ of synthesis system.

The function fitting of the nuclear pulse signal frequently uses the uni-exponential and bi-exponential models [15]. In this work, the original pulse signals are characterized by the uni-exponential model and the discrete expression to perform the characterization is shown in

* Corresponding author.
*E-mail addresses:* 24829500@qq.com (G. Zeng), 22105653@qq.com (J. Yang).

http://dx.doi.org/10.1016/j.nima.2017.03.049
Received 18 September 2016; Received in revised form 7 March 2017; Accepted 26 March 2017
Available online 28 March 2017

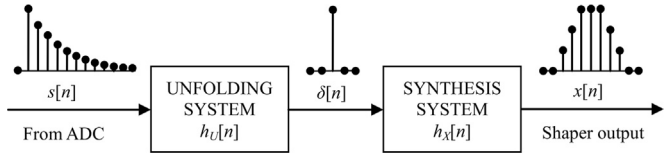


**Fig. 1.** Functional block diagram of a trapezoidal pulse shaping system using the unfolding-synthesis technique.

Eq. (1).

$$s[n] = Aa^{n-n_0}u[n-n_0] + (B+Cn)u[n] \quad (1)$$

Where $a=exp(-T_S/\tau_O)$, $T_S$ is the ADC sampling period, $n_O$ is the initial position of the pulse signal, and $u[n]$ is the discrete step signal. In order to facilitate the analysis of the baseline restoration technique, Eq. (1) contains an initial DC offset, $B$, and a baseline shift, $Cn$, at a particular rate. The baseline shift sections have led to an imbalance of the bilateral baseline, which can be used to analyze the baseline drift. First, an analysis must be performed on the influence of the deconvolution system on the baseline of the original pulse signal. Eq. (2) shows the recursive difference equation of the deconvolution system.

$$v[n] = s[n]-as[n-1] \quad (2)$$

Eq. (1) is substituted into Eq. (2) to derive the output, $v[n]$, of the deconvolution system.

$$v[n] = A\delta[n-n_0]+B\delta[n]+(1-a)(B+Cn)u[n-1] \quad (3)$$

Eq. (3) show that $v[n]$ still contains a baseline DC offset and a baseline drift. As a result, the deconvolution system cannot restore the baseline, and the baseline is only reduced. In addition, $v[n]$ also includes two unit impulse signals. The $A\delta[n-n_O]$ is from the deconvolution of the pulse signal, and the $B\delta[n]$ is from the deconvolution of the step signal (DC offset). The unit impulse signals are synthesized to the expected shape through the pulse synthesis system, but the baseline DC offset and the baseline drift are not clearly identified. Thus, the analysis of the convolution of $v[n]$ and the transfer function, $h_X[n]$, is shown in Eq.(4).

$$\begin{aligned} x[n] &= v[n]*h_X[n] = \sum_{k=0}^{N-1} v[k]h_X[n-k] = \sum_{k=0}^{N-1} v[n-k]h_X[k] \\ &= A\sum_{k=0}^{N-1}\delta[n-n_0-k]h_X[k]+B\sum_{k=0}^{N-1}\delta[n-k]h_X[k]+(1-a) \\ &\times\left\{B\sum_{k=0}^{N-1}u[n-k-1]h_X[k]+C\sum_{k=0}^{N-1}nu[n-k-1]h_X[k]\right\} \end{aligned} \quad (4)$$

Where $N$ is the number of points used for the pulse shaping. The convolution is divided into four parts. The two parts on the left are the impulse responses $h_X[n-n_O]$ and $h_X[n]$. The third part is equivalent to a single integral of $h_X[n]$, and the fourth part is equivalent to double integral of $h_X[n]$. The last two parts directly determine the change of the baseline through the pulse shaping. Selecting $a$=0.988, $B$=0.2 and $C$=0.001 to analyze the integral of the pulse shaper's transfer functions, such as the trapezoidal shaper, the BZA trapezoidal shaper and the SZA trapezoidal shaper. The shaping time is 15μsec and the corresponding flat-top time is 1μsec.

Fig. 2 shows the integral of the trapezoidal shaper's transfer function, which generates a stable baseline DC offset through a single integral of its transfer function while the double integral of its transfer function generates a baseline drift. The baseline variations of the input pulse signal have the same influence on the baseline of the trapezoidal shaper. The baseline of the BZA trapezoidal shaper is stable and has no DC offset through the single integral, but the double integral of its transfer function generates a stable baseline DC offset. Thus, the BZA trapezoidal shaper cannot restrain the baseline drift. However, the baseline of the SZA trapezoidal shaper is stable through both single integral and double integral, so it effectively can both restore the baseline and restrain the baseline DC drift. In addition, Fig. 2 shows the normalized amplitude, and it can be observed that the baseline fluctuations of the SZA trapezoidal shaper are the smallest among these shapers.

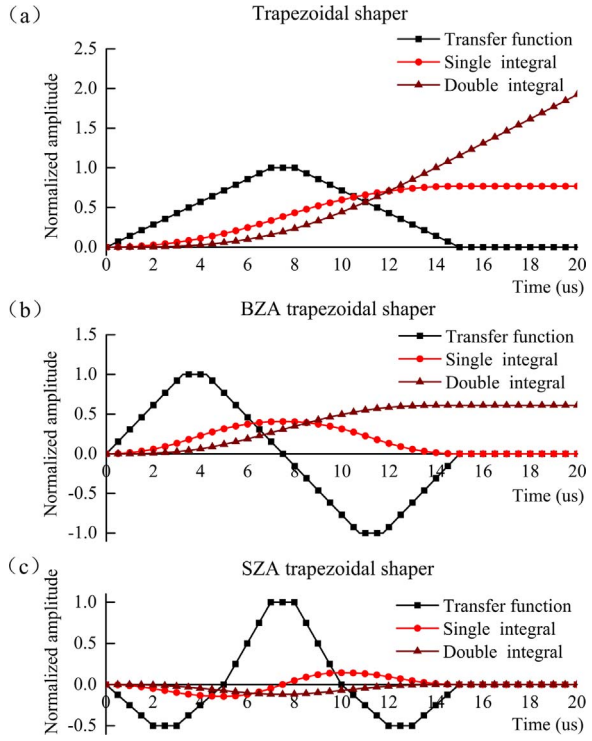


**Fig. 2.** The integral of the transfer functions (a)the results of the trapezoidal shaper, (b) the results of the BZA trapezoidal shaper, and (c)the results of the SZA trapezoidal shaper.

## 3. Recursive algorithm of the SZA trapezoidal shaper

The algorithm of the SZA trapezoidal shaper is based on the recursive difference equations in the time domain [16], as shown in Eqs. (5)–(11). Since the recursive algorithm is beneficial to reduce the multiplication operations, it can output the results in real-time.

$$v[n] = s[n]-a\bullet s[n-1] \quad (5)$$

$$p[n] = v[n]-v[n-l] \quad (6)$$

$$q[n] = p[n]-p[n-l-m] \quad (7)$$

$$r[n] = r[n-1]+q[n] \quad (8)$$

$$x[n] = x[n-1]+r[n] \quad (9)$$

$$y[n] = x[n]-x[n-2l-m] \quad (10)$$

$$z[n] = y[n-2l-m]-y[n] \quad (11)$$

Where $l$ is the hypotenuse points of the isosceles trapezoid and $m$ is the flat-top's points. When $m$=0, the shapebecomes an SZA triangle. Fig. 3 shows the recursive method of the SZA trapezoidal shaper, which can

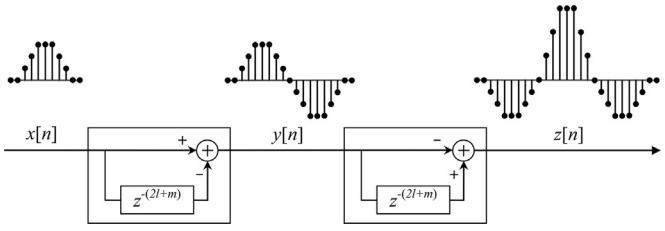


**Fig. 3.** The recursive method of the SZA trapezoidal shaper.

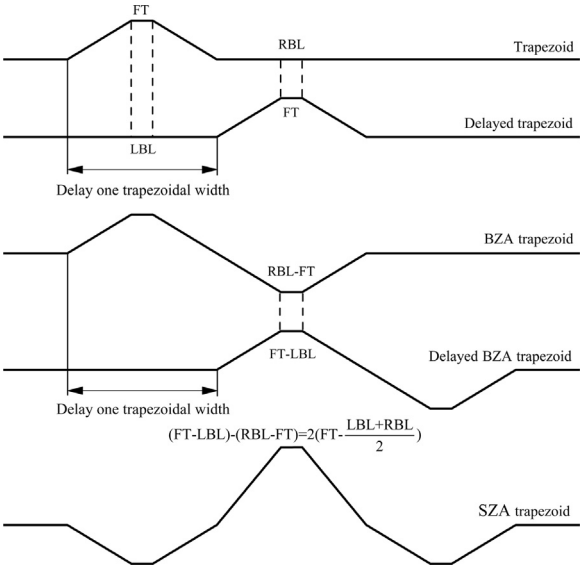


**Fig. 4.** The method of the balance technique of the SZA trapezoidal shaper.

also be applied to the similar pulse shapers, such as the SZAcusp-like shaper.

The diagram of the recursive method can be used to analyze the balance technique of the baseline drift in the SZA trapezoidal shaper. The trapezoid's flat-top (FT), left baseline (LBL) and right baseline (RBL) are marked in Fig. 4. The unipolar trapezoid shaper need a baseline estimator to accurately extract the height of the trapezoid's flat-top. However, the baseline of the BZA pulse shaping can be restored automatically. The height of its left positive trapezoid is equivalent to FT-LBL, and the height of its right negative trapezoid is equivalent to RBL-FT. But if the differences of the bilateral baselines are large due to the baseline drift, the baseline deduction of the positive and negative trapezoids are not equal so that the amplitude of the two trapezoids would be significantly different. The SZA trapezoid is equivalent to a BZA trapezoid subtracting its delay of one trapezoidal width. The height of the middle flat-top of the SZA trapezoid is equivalent to the flat-top of the original trapezoid subtracting the average of the bilateral baseline, namely, FT-(LBL+RBL)/2. Even if the difference of the bilateral baseline is large, it can reduce the middle trapezoid's baseline fluctuations by the balance of the bilateral trapezoids.

## 4. Implementation in FPGA

The recursive difference equations of the SZA trapezoidal shaper can be easily implemented in FPGA. The shift registers are used to realize the signal delay and the adders are used to achieve the integral operations. This method avoids excessive multiplication in the convolution and can output the result in real-time. The nuclear pulse signal of the detector must be preprocessed through the signal conditioning circuits and then digitized by the high-speed ADC for digital signal processing in the FPGA. High-speed ADC selects the 8-Bit, 32 MSPS sampling, AD9280, and the FPGA selects the Altera's low-cost EP4CE series. The logic diagram of the algorithm in the FPGA is shown in Fig. 5.

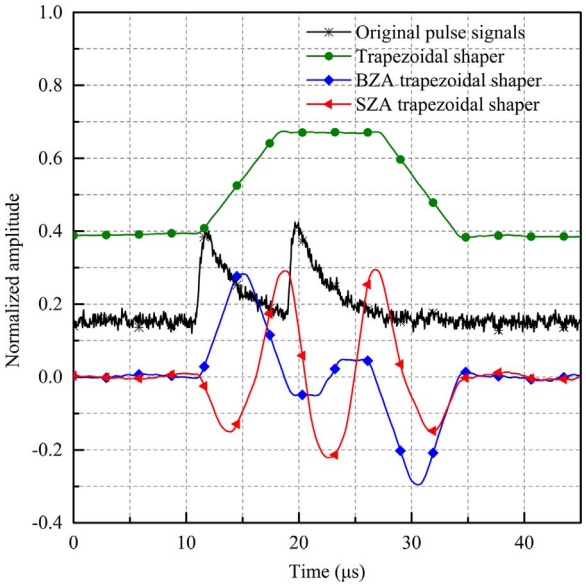


**Fig. 6.** The actual test results using the three pulse shaping methods.

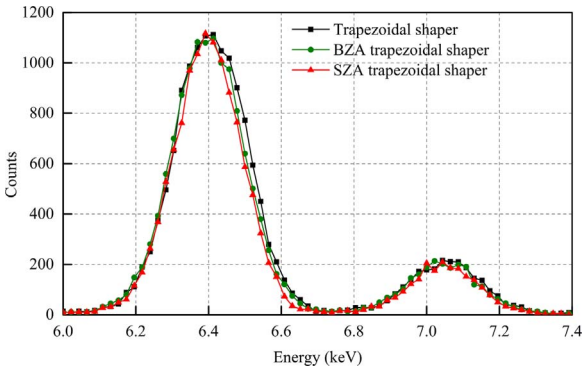


**Fig. 7.** The measured energy spectrums of iron's characteristic X-ray at low count rates and the photon count rates is 10 kcps.

The parameter $a=exp(-T_S/\tau_O)$ in the difference equations is a constant float-point type. Float-point operations in the FPGA should be avoided in order to improve the operating speed. This parameter can be converted into a fraction, which can have integer multiplication and integer division operations. In addition, a suitable time constant, $\tau_O$, should be selected to guarantee that the baseline has no undershoot or trails. The optimal time constant can be determined by observing whether the flat-top is parallel to the baseline [16,17]. However, the flat-top judging method is not readily performed in the case of serious ballistic deficits [1], since the flat-top is a gradually rising and then stable process. Since the poor time constant would cause the different amplitudes of two symmetrical trapezoids at the bottom of SZA trapezoidal shape, an optimal time constant can be determined by judging whether the amplitudes of the two trapezoids are equal.

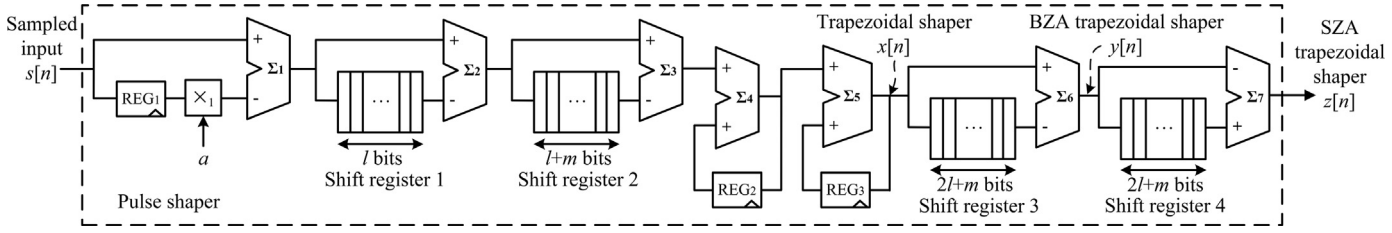


**Fig. 5.** The logic diagram of the SZA trapezoidal shaper algorithm in the FPGA.

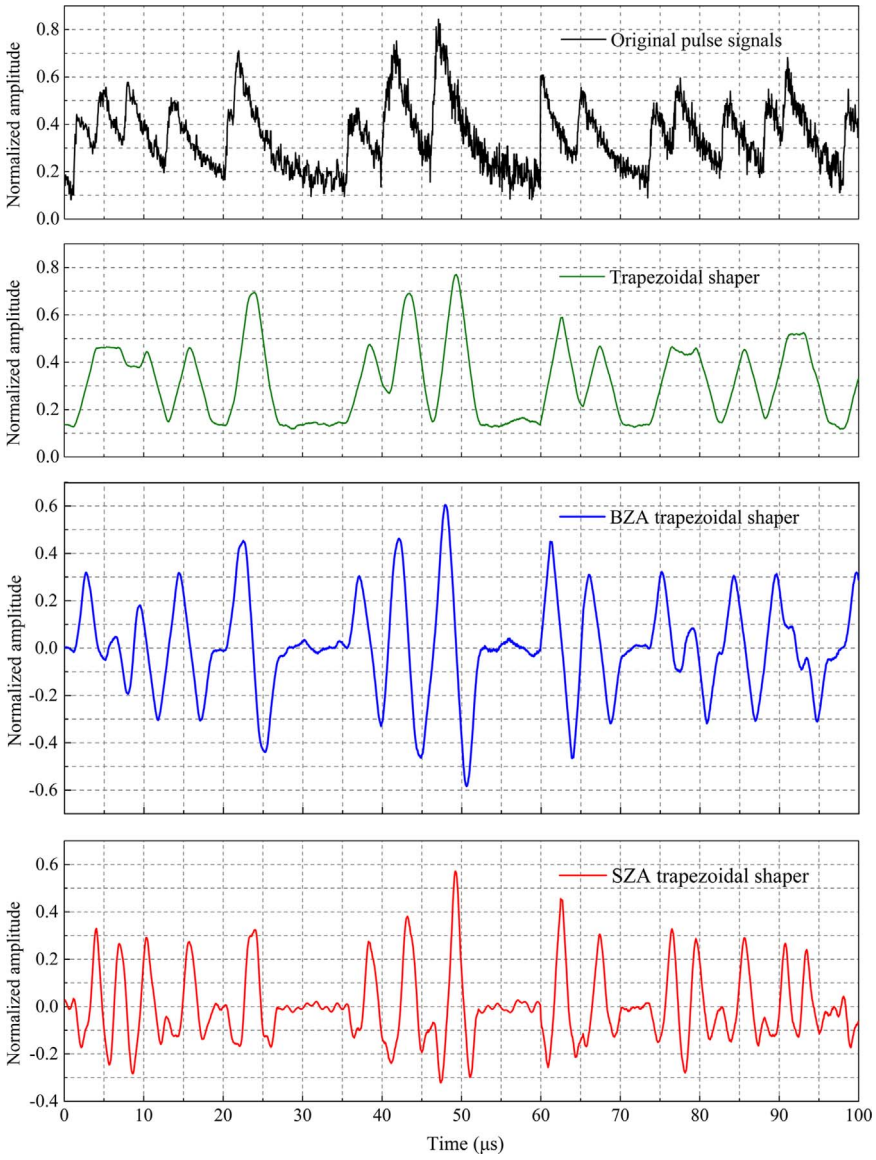


**Fig. 8.** The actual test results using the different pulse shaping methods at high count rates.

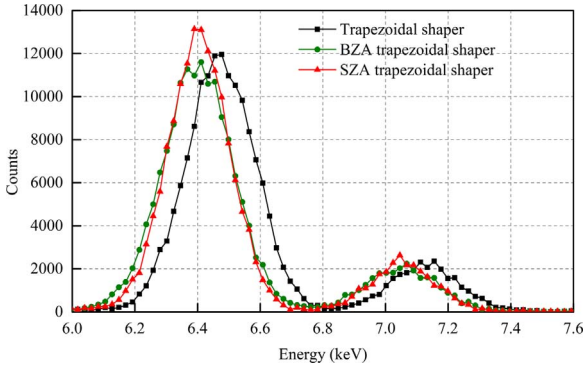


**Fig. 9.** The measured energy spectrums of iron's characteristic X-ray at high count rates and the photon count rates is 94 kcps.

## 5. Experiments and discussion

In this experiment, the pulse signals are obtained through the X-Ray irradiation of iron. And the X-Ray are generated by the MOXTEK's 50 kV Monoblock X-ray Source (TUB00083-AG1). The energy of the iron's characteristic X-ray was detected by a MOXTEK's XPIN-XT Si-PIN detector (diode active area: 13 $mm^2$), and this Si-PIN detector can achieve a full width at half maximum (FWHM)≤230 eV ($Fe^{55}$, 5.9 keV @−35 °C, 8 μ s shaping time). The output of the Si-PIN detector is preprocessed through a differential amplifier, and then a CR (C=6.8uF and R=470 Ω) circuit is used to generate the exponential pulse signals. In order to verify the effect of this algorithm in the FPGA hardware, the SignalTap logic analyzer is used to obtain the data in the FPGA memory through the joint test action group (JTAG) hardware debugger in real-time.

Fig. 6 shows the original pulse signals with 20 MSPS sampling rates and the corresponding pulse shaping when the high voltage of the X-Ray tube is 30 kV, and its current is 5 μA. The amplitude of the original pulse signals is approximately 550 mV, the pulse width is approximately 10 μ s, and the ripple of baseline is approximately 50 mV. The shaping time is 15μsec and the corresponding flat-top time is 1μsec. The trapezoidal shaper and the BZA trapezoidal shaper were unable to distinguish the pile-up of the first two pulse signals since their respective methods to perform pile-up rejection are complex. However, the two pulse signals can be correctly distinguished with the SZA trapezoidal shape since the pile-up rejection and amplitude extraction are simplified. A triggered threshold, being greater than zero, is set up to capture the pulse. All signals, being greater than this

threshold, can be directly used for peak extraction without the need for baseline extraction. This method is similar with the three zero-area digital filters for peak recognition in spectral data analysis [18]. The dead signals are discarded, which are the peak intervals that are less than half of the shaping time constant.

As shown in Fig. 7, the corresponding energy spectrums of iron's characteristic X-ray are respectively obtained from the tests of the trapezoidal shaper with a baseline restoration technique (a moving average, 20 sampling points window), the BZA trapezoidal shaper and the SZA trapezoidal shaper using the same data. Compared to the traditional trapezoidal shaper, the SZA trapezoidal shaper improved the FWHM of the Kα characteristic peak at 6.403KeV from 237 eV to 216 eV. In addition, the FWHM after the BZA trapezoidal pulse shaping is 235 eV, and it is almost the same as trapezoidal shaper at the low count rates.

In order to test the performance of the SZA trapezoidal shaper at high count rates, we increase the current of the X-Ray tube from 5 μA to 50 μA and reduce the shaping time from 15 μ s to 5 μ s. As can be seen in the Fig. 8, the baseline also have a great fluctuation due to the serious pulse pile-up. Since the traditional trapezoidal shaper cannot eliminate this drift instead of amplifying the baseline DC offset, so the baseline after the trapezoid pulse shaping is also fluctuant remarkable. In this case, the baseline extraction of the trapezoid pulse shaping is not accurate, especially the subsequent baseline fluctuation in multiple pulse pile-up. Even if using the baseline filter, the flat-baseline can only be detected in a small time interval. Although the BZA trapezoidal shaper can restore the baseline, the baseline drift probably cause different amplitudes for its positive and negative trapezoid. In addition, the biggest drawback of the bipolar pulse shaper is that the negative trapezoid of the previous pulse easily overlaps the positive trapezoid of the latter pulse, causing to the latter shape's amplitude to change, so the dead time of the BZA shaper is very small, so its pile-up rejection approach is very complex when the pulse pile-up is serious. For the SZA trapezoidal shaper, the baseline restoration has been carried out in the pulse shaping algorithm. It is no need for baseline extraction, and the peak can be extracted directly and the dead time are only judged by the peak's time interval. Furthermore, the SZA trapezoidal shape can also restrain the baseline drift through the bilateral trapezoids balancing the middle trapezoid's baseline.

For the three pulse shaping approach at the high count rates, the measured energy spectrums are shown in Fig. 9. After using the unipolar trapezoidal pulse shaping, the Kα and Kβ characteristic peaks shift to the right and the peaks are asymmetric. Meanwhile, the FWHM of the Kα characteristic peak is widened from 237 eV to 257 eV. For the BZA trapezoidal shaper, its count rates of the characteristic peak is the lowest due to its large dead time, as well as its worst FWHM, 262 eV. However, the SZA trapezoidal shaper maintains the characteristic peak position. Although its energy resolution deteriorated, its FWHM of the Kα characteristic peak being 225 eV, it can still obtain optimal energy resolution and the remarkable count rates of the characteristic peak.

As can be seen from the energy spectrums, in the case of the low count rates, the signal-to-noise ratio (SNR) of the SZA trapezoidal pulse shaping is improved by using a long shaping time to achieve a better baseline filtering effect and a higher energy resolution than the traditional trapezoidal pulse shaping. In the case of high count rates, this shaper's clear pile-up rejection approach and baseline restoration technique guarantee the symmetrical photoelectric peak and its accurate position, as well as a great energy resolution. Although the SZA trapezoidal shaper can restrain the baseline shift effectively especially a large baseline fluctuation, its SNR is not better than the trapezoidal shaper in the same shaping time, especially the small shaping time at higher count rates. In order to show the advanced performance of the SZA shaper in this case, the smaller width of the bilateral trapezoid of the SZA shaper as well as a the better SZA cusp-like shaper can be used to improve their SNR.

## 6. Conclusions

This study presents an SZA trapezoidal pulse shaping algorithm based on the recursive difference equations in the time domain. The zero-area method of the SZA trapezoidal pulse shaper can be used for baseline restoration, which can eliminate the baseline DC offset of the pulse signals, while the symmetrical method can restrain the baseline drift. This algorithm is implemented in a real-time hardware system based on high speed ADC and FPGA. Lastly, a low SNR signals of iron's characteristic X-ray are detected with a Si-PIN detector. The test results show that the SZA trapezoidal shaper reduces the influence of the baseline drift on the amplitude extraction to improve the energy resolution. In addition, it simplifies the methods of pileup rejection and amplitude extraction. This baseline restoration technique also reduces the influence of noises and temperature on the pulse baseline, and improves the accuracy and stability of the long-term operation in nuclear spectrometry systems. In future work, the sampling rates should be improved to increase the number of points for the pulse shaping in order to improve the pulse throughput. A greater resolution of the ADC is also needed to improve the energy resolution further.

## Acknowledgements

Funding: This work was supported by the National Natural Science Foundation of China [Grant no. 41474159]; the Sichuan Youth Science & Technology Foundation [Grant no. 2015JQ0035]; and the Key Laboratory of Applied Nuclear Techniques in Geosciences Sichuan [Grant no. gnzds2014006].

## References

[1] V.T. Jordanov, G.F. Knoll, Nucl. Instrum. Methods Phys. Res. A 345 (1994) 337.
[2] V.T. Jordanov, Nucl. Instrum. Methods Phys. Res. A 505 (2003) 347.
[3] A.I. Kalinin, V.A. Bednyakov, Nucl. Instrum. Methods Phys. Res. A 538 (2005) 718.
[4] A. Geraci, I. Rech, E. Gatti, et al., Nucl. Instrum. Methods Phys. Res. A 482 (2002) 441.
[5] X. Wen, Y. Wei, IEEE Trans. Nucl. Sci. 53 (2006) 3865.
[6] G. Gerardi, L. Abbene, Nucl. Instrum. Methods Phys. Res. A 768 (2014) 46.
[7] H. Li, C. Wang, H. Baghaei, et al., IEEE Trans. Nucl. Sci. 57 (2010) 550.
[8] A. Pullia, G. Gritti, G. Ripamonti, IEEE Trans. Nucl. Sci. 44 (1997) 331.
[9] A. Pullia, A. Geraci, G. Ripamonti, Nucl. Instrum. Methods Phys. Res. A 439 (2000) 378.
[10] A. Pullia, G. Ripamonti, Nucl. Instrum. Methods Phys. Res. A 391 (1997) 301.
[11] V. Esmaeili-sani, A. Moussavi-zarandi, et al., Nucl. Instrum. Methods Phys. Res. A 665 (2011) 11.
[12] V. Esmaeili-sani, A. Moussavi-zarandi, et al., Nucl. Instrum. Methods Phys. Res. A 694 (2012) 113.
[13] M. Kafaee, A. Moussavi-Zarandi, J. Korean Phys. Soc. 68 (2016) 960.
[14] V.T. Jordanov, Nucl. Instrum. Methods Phys. Res. A 805 (2016) 63.
[15] G.F. Knoll, Radiation Detection and Measurement, 3rd ed., Wiley, New York, 2000.
[16] J. Lanchares, O. Garnica, et al., Nucl. Instrum. Methods Phys. Res. A 727 (2013) 73.
[17] A. Regadio, S. Sanchez-Prieto, et al., Nucl. Instrum. Methods Phys. Res. A 735 (2014) 297.
[18] F. Janssens, J.P. Francois, Anal. Chem. 63 (1991) 320.